NUMERICAL AND EXPERIMENTAL STUDY OF THE EFFECT OF CIRCUMFERENTIAL GROOVES ON HPC LAST STAGE PERFORMANCE

V.I. Mileshin, A.M. Petrovitchev, S.I. Baeva, V.V. Zhdanov
Central Institute of Aviation Motors (CIAM)

Abstract

High pressure ratios in advanced axial compressors lead to a decrease in height of the flow path and, consequently, a decreased blade height in HPC last stages. The blade tip clearance can't be reduced relatively to the blade chord length or height by the same relative value as in first stages. Moreover, HPC operation in transient conditions can cause an increase in tip clearances, so that clearances in last stages can exceed normal values. This may affect the operating range and characteristics of the compressor as a whole. Circumferential groove casing treatments can be used to compensate for negative effects associated with an increase in tip clearances.

The test unit used in this work is a D-77M stage – the large-scale (1 m) model of the HPC last stage designed for studies of flow specifics in axial stages with a big hub-to-tip ratio equal to 0.925. It consists of 3 blade rows: inlet guide vanes (IGV) with 90 vanes (ZIGV), which provide the same flow swirling as in an actual compressor, a rotor with 82 blades (ZR) and a tandem stator with 134+134 vanes (ZSII). The D-77M stage has the following design parameters: mass air flow 15.4 kg/s; tip speed 264 m/s; total pressure ratio 1.24.

The purpose of the circumferential grooves is recovery the stall margin, pressure ratio and maximum level of efficiency, which have decreased due to an increase in the tip clearance. Two values of the tip clearance are studied: a) 0.4 mm – design value of the tip clearance, and b) 0.8 mm – increased value of the tip clearance. Dimensions and distances between the grooves are chosen in view of their subsequent manufacturing. Various configurations of casing treatments with different number of grooves located in the area of the leading edge or over the entire rotor chord are numerically studied in this work. This choice can be explained by the fact that vortex caused by leakages in the tip clearance is located in the area of the leading edge, and its intensity considerably increases with an increase in the tip clearance. Grooves located directly in the area of the leading edge split the main vortex into a number of small vortices and decrease its intensity, but similar grooves located near the trailing edge have a negligible effect on flow. Nevertheless, the casing treatment in the configuration with 6 grooves located over the entire blade chord results in max. increase in efficiency. The circumferential grooves show a positive effect on flow at design rotational speeds as well as decreased rotational speeds in the D-77M stage. Calculated and experimental characteristics of the D-77M stage with a smooth flow path were compared.

Nomenclature

Thermodynamic and gas-dynamic parameters:

P_T – total pressure, Pa;
T_T – absolute total temperature, K;
G – mass air flow, kg/s;
π^* – total pressure ratio;
$\eta^*_{ad} = H_{ad}/H_Z$ – adiabatic efficiency.

Geometrical parameters:

D, R – diameter, radius, m;
C_x – axial chord;
$\bar{d}$ – hub-to-tip ratio;
d_{tip} – tip clearance, mm;

z – number of circumferential grooves in CT;
Z – number of blades.

Kinematic parameters:
n – rotational speed, r.p.m.;
u – tip speed, m/s;
C – absolute flow velocity (in the fixed coordinate system), m/s;
W – relative flow velocity.

Indices and Abbreviations:
IGV – inlet guide vanes;
R – rotor;
SII – tandem stator;
CT – casing treatment;
t – tip;
h – hub;
cor – corrected.

1 Introduction

In connection with the development of a new high-pressure HPC family with ultra-high pressure ratio $\pi_c^*=27$ and number of stages $z=10\div11$ studied by Aspi Wadia et al. in [1], P.S. Prahst et al. in [2] and D.P. Lurie et al. in [3] the effect of the tip clearance in HPC last stages is of particular importance shown by V.I. Mileshin in [4,5]. An increase in the tip clearance in comparison with a design value leads to a noticeable degradation of HPC performance. The negative effect of the tip clearance can be compensated by abradable coatings on the HPC casing inner surface. However, as a result of unstable transient conditions, a casing ovalization, and an inlet flow nonuniformity observed in the process of HPC operation, the coating height decreases that leads to an increase of the tip clearance and an additional degradation of HPC performance demonstrated by Mileshin et al in [6,7,8].

The effect of circumferential grooves on characteristics of a typical HPC middle stage with an increased tip clearance is studied by V. Mileshin et al. in [9]. It is shown that an increased tip clearance causes a decrease in stall margin, and the use of circumferential grooves makes possible to suppress this negative effect. Grooves reduce mass flow in the tip clearance and shift the leakage vortex deeper into the blade channel, thereby positively affecting the stall margin.

Circumferential grooves can exert a considerable influence on compressor performance; moreover, they are not difficult for manufacturing. Recently, a numerous number of works have been completed to study their associated flow mechanism. It is well known that grooves exert an effect on leakage flow in the tip clearance by suppressing its rolling up, as shown by M. Govardhan et al. in [10]. Benefits of circumferential grooves for increasing the stall margin are verified in the numerical study by Juan Du et al. in [11]. It is emphasized by Wilke I. et al. and by Hah C et al. in [12-14] that the physical effect of grooves consists in a considerable reduction of blockage at the tip and a decrease of leakage vortex rolling up in the tip region of the blade passage.

The influence of a shape and a position of one groove on efficiency and stall margin were studied by Rabe D.C. and Hah C. in [15]. Two types of grooves were studied: a triangular groove with upstream bevel angle, which is located in the area of the blade leading edge – it has a positive effect on stall margin and slightly decreases the efficiency; and a trapezoidal groove, which is located in the area of the trailing edge – it increases efficiency and has a negative effect on stall margin. It is also shown that effects of each of the grooves are independent, and their combination makes possible to compensate for losses if used individually.

The study is completed with an increased rotor tip clearance. It is shown by Shabbir A. and Adamzyk J.J in [16] that due to changes in the flow field caused by an increased tip clearance, the positive effect of casing treatments is not the same as found for the nominal clearance. It is reported that an axial position of grooves is an important parameter.

G. Goinis et al. in [17] looked at the effect of the position of a casing treatment consisting of six rectangular grooves. Three CT positions are analyzed: 1) all grooves are above the rotor; 2) all grooves are shifted downstream; 3) all grooves are shifted upstream. The maximum increase in stall margin is found in the first case

- all grooves are located in the area above the rotor (10.3%).

The effect of circumferential grooves and bending of rotor blade tips on stall margin is studied by M. Rolfes et al. in [18]. It is shown that stall margin can be additionally improved by blade bending.

A slot-groove hybrid casing treatment is studied by Hao Guang Zhang et al. in [19]. The slots are located at the leading edge, and circumferential grooves – at the trailing edge. As a result of calculations and tests, it is found that effects of both casing treatments can be identified. It is shown that changes in stall margin are caused by an influence of the casing treatment on a trajectory of the leakage vortex. The more powerful the vortex, the more visible its trajectory tends to the blade suction side. A decrease in efficiency is caused by an increase in entropy production in slots and grooves as well as losses caused by flow induced by these slots.

This work was carried out in an effort to develop methods and technologies aiming at an improvement the last compressor stage performance (including an increase in stall margins), as well as a reduction of sensitivity of last compressor stage performance to changes in rotor tip clearances. Similar problems were studied earlier by Cevik, M. et al. in [20] This paper presented the development of a novel casing treatment to reduce compressor performance and stall margin sensitivities to tip clearance increase. The casing treatment design consists of sawtoothshaped circumferential indentations placed on the shroud over the rotor with a depth on the order of the tip clearance size. Further simulations showed that this casing treatment can be combined with desensitizing blade design strategies developed by Erler, E. et al. in [21] to further reduce tip sensitivity and reduce/eliminate/reverse nominal performance penalty.

2 Test unit

The D-77M stage (see Fig. 1) is a large-scale model of a HPC last stage designed for studies of flow in axial stages with a big hub-to-tip ratio ($\bar{d}$=0.925); it consists of three blade rows: IGV with 90 vanes (Z_{IGV}), a rotor with 82 blades (Z_R) and a tandem stator with 134+134 vanes (Z_{SII}). The stage has the following design parameters: G=15.4 kg/s; u=264 m/s; π^*=1.24.

a) Rotor of the D-77M stage

b) Outlet casing

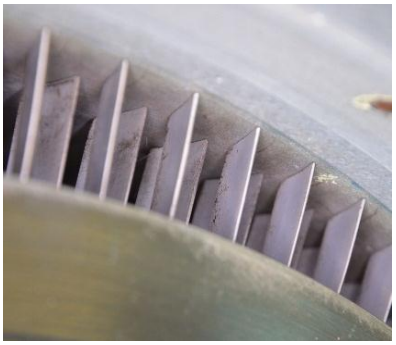

c) Tandem stator

Fig. 1. D-77M stage

The D-77M stage configuration is mainly designed to study the effect of different types of casing treatments on performance of a typical HPC last stage with an option to change rotor tip clearances.

Two values of tip clearances over the rotor were studied in this work: d_{tip} = 0.4 mm (0.9% of tip chord) - normal clearance and d_{tip} = 0.8 mm (1.8% of tip chord) - increased clearance. Changes of the tip clearance in the D-77M stage were provided by changing the diameter of the outer casing above the rotor.

A set of removable casing rings were manufactured to change the tip clearance and the number of grooves in the casing treatment,

including casings with a smooth flow path and with circumferential grooves when the number of grooves (z) was equal to 4 or 6.

Due to machining limitations, tests were performed only for the CT with four grooves without the tandem stator in the D-77M stage. Tests with the tandem stator will be performed at the next stage of the work.

The D-77M stage was tested at the CIAM's UK-3 test facility equipped with a torsion torque meter falling into Class 0.2 (ET60, «Torquemeters» company) with 500-Nm sensor.

Work expended for an increase in total pressure in the D-77M stage is calculated as work expended in rotation (estimated on the basis of measured torque) minus work in friction of bearings and disks. Friction work in the disk and bearings was pre-determined in "blades off" tests of the stage.

Lubricating oil temperature was supported in tests within 30 ± 10°C.

To make total pressure measurements, three 7-point total pressure rakes with flow deflectors providing nonresponsiveness of measurements to changes in the velocity direction (up to ± 30°) were installed at the rotor outlet (phase 1) and at the stator outlet (phase 2). The IKD-27Df sensors were used as pressure transducers; their measurement accuracy was max.± 0.3% of a full scale. Before testing a new stage assembly, the sensors were calibrated using DPI-620 instruments to provide the required measurement accuracy. A device providing slow stator rotation was switched ON during measurements for more accurate estimations of an average total pressure value.

Two 7-point total temperature rakes were installed for temperature measurements. Air flow was measured by a flow metering orifice after metrological certification in accordance with OST 1 02555-85. Air flow measurement accuracy was max. ± 0.5% of a measurable value.

The configuration of the measurement system and the test procedure provided max. ± 0.5% error in estimations of D-77M stage efficiency.

2 Numerical model

Numerical flow simulation was provided by the software package for solving the Reynolds averaged steady and unsteady 3D Navier-Stokes equations (RANS, URANS) [22,23].

The simulation process was completed in two phases. At first, two rows (IGV and Rotor) were used for a more detailed analysis of the effect of circumferential grooves on the rotor. After that the tandem stator was taken into account in calculations, and similar studies were performed for the full D-77M stage.

Through-flow calculations of three-dimensional viscous flow in blade rows in the «Mixing plane» approximation were completed at the first phase. Flow was steady in the coordinate system rotating with each blade row. Unsteady flow fields for the incomplete stage were found by a nonlinear harmonic method (NLH) allowing simulation of one blade passage per row without using "mixing plane" interface [24]. The basic idea of this method lies in the fact that disturbances making flow unsteady are recorded as time-averaged values and then expanded into Fourier series. By presenting the unsteady Navier-Stokes equations in the frequency form, we derive transfer equations for each frequency. The condition of solution equality on both sides should be observed at the stator-rotor interface. The main goal is to get continuous unsteady flow through the interface. The number of harmonics is limited, and, consequently, continuity can't be strictly reproduced, but the difference in numerical results decreases with an increase in the number of harmonics. In this study, the number of harmonics was taken equal to 3.

A two-parameter model of turbulent viscosity (SST) with wall functions was used without boundary layer transition model. Solutions were found by the Jameson's finite-difference scheme in the second-order approximation in space and time.

Unfortunately, the SST model was unable to make calculations for IGV+R+SII configuration because it was sensitive to artificial separation areas in the tandem stator

which were generated at the interim steps of convergence process. In this case, k-ε model proved itself as more stable, which pre-determined its choice for 3D viscous flow calculations for the stage in IGV+R+SII configuration. For the full compressor stage the study was limited only by the «Mixing plane» approach.

A block-structured grid was used in calculations. Only one blade passage per row was simulated. The grid was constructed by the automatic grid generator (Fig. 2-4) [23]. At the first phase, the computational domain consisted of 16 grid blocks in blade channels (1,627,508 cells) and 4 or 6 blocks in the casing treatment (121,841 cells per a groove with a quadrangular cross-section, 104,673 cells per a groove with a triangular cross-section). Investigation of final mesh size was performed, the results of which are presented in the Table below. At the second phase of the study the mesh density was increased twice; the total computational domain was divided between 28 grid blocks (4,959,728 cells) in blade channels and 4 or 6 blocks in the casing treatment (121,841 cells per a groove with a quadrangular cross-section, 104,673 cells per a groove with a triangular cross-section) y^+=0.879. General view of the computational domain is shown in Fig. 2-Fig. 4. The mesh of O-H type with 17 radial cells was used in the tip clearance which satisfies with best practice recommendations by Van Zante at al. [25].

Table Results of final mesh size study

Mesh cells	G_{cor}	Δ, %	π^*	Δ, %	η^*_{ad}	Δ, %	ΔSM, %	Δ, %
773140	12.93	-0.69	1.249	-0.16	0.9084	-0.88	6.1	-3.4
1627508	13.02	0	1.251	0	0.9165	0	9.6	0
3168808	13.03	0.08	1.251	0	0.9182	0.19	13.5	3.9

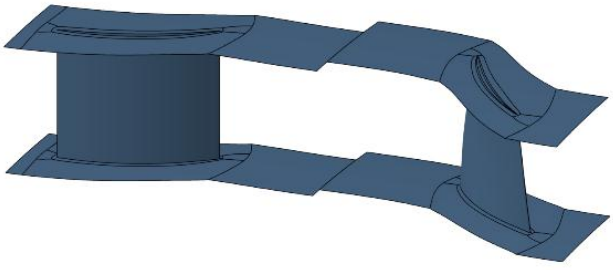

Fig. 2. Computational domain for IGV +R

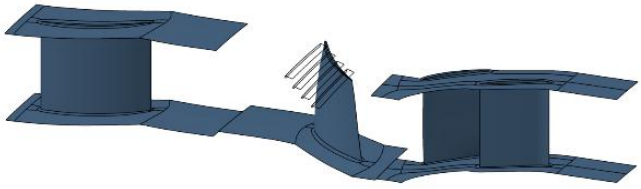

Fig. 3. Computational domain for IGV +R+SII

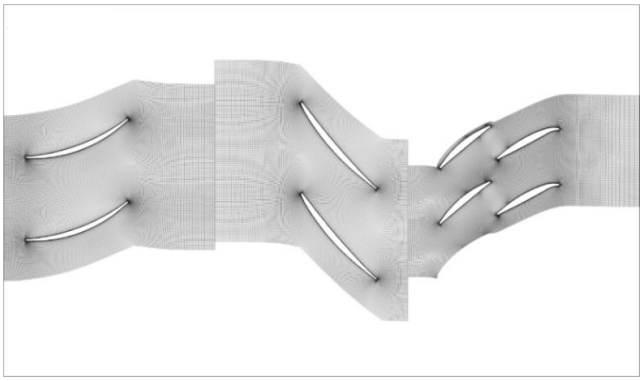

Fig. 4. Finite-difference grid in the blade channel section in the D-77M stage

Viscous flow calculations were based on corrected parameters at the inlet: TT=288.15K, PT=101325Pa at n=100% corresponding to 5042 r.p.m. Because of a short inlet duct, the boundary layer at the hub and at the tip was thin making possible to specify total pressure and total temperature at the inlet to be constant across the section. The inlet turbulence value was 5.15%, i.e. was in full compliance with test conditions. The condition of radial flow equilibrium was used in the outlet section; static pressure at the tip was fixed. Conditions of flow "no slip" and zero heat transfer were specified on solid surfaces. Two values of rotor tip clearances were studied: d_{tip} = 0.4 mm - design height of the tip clearance and d_{tip} = 0.8 mm - increased height of the tip clearance.

Based on results found by the studies [17], the triangular shape of the groove cross-section was chosen; 6 grooves were located over the entire blade chord. The width of the triangular groove was 3 mm (10.0% of axial chord); the other dimensions see in Fig. 5a. Later on, based on capabilities of the manufacturing process for this type of casing treatment, the groove was re-designed with a truncated cross-section and the number of grooves was reduced (Fig. 5b). Grid blocks corresponding to circumferential grooves had the same periodicity as the rotor blade

channels (Z = 82 blades). Grooves were modeled as separate rotating computational sub domains connecting with the flow part using full non-matching boundary connection.

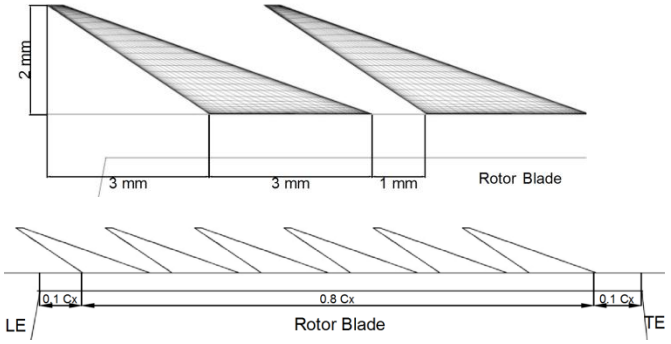

a) For the numerical model

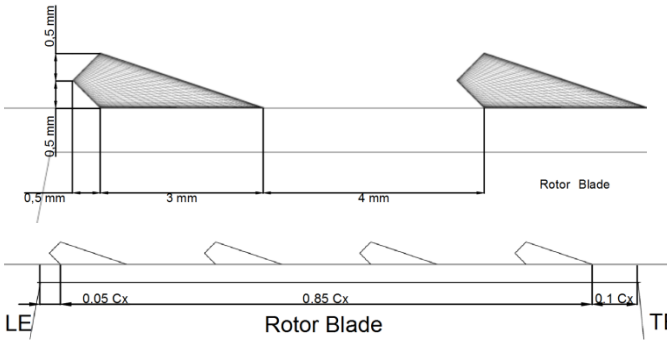

b) With account of manufacturing recommendations

Fig. 5. Configuration of the CT with circumferential grooves

To find speed lines, back pressure at the outlet slowly increased until reaching non-convergence of the solution.

4 Calculated data

As a result of numerous calculations, integral characteristics shown in Figures 6-8 were found.

Figure 6 shows integral characteristics of the D-77M stage without the tandem stator found experimentally and numerically using the "mixing plane" interface. Casing treatments of investigated configurations had no visible effect on integral characteristics of the stage at nominal tip clearance. Twice as large tip clearance resulted in a noticeable degradation of parameters of D-77M stage in smooth wall configuration (a decrease in efficiency by 1.5% and a decrease in stall margin by 7%). Application of casing treatments of investigated configurations made possible to restore stall margins and increase efficiency by 0.8%. Comparison of calculated data (see Fig. 6) showed a good agreement for total pressure ratio (π^*) and efficiency (η^*_{ad}). For example, maximum deviation for efficiency was 0.5%, and maximum deviation for total pressure ratio was 0.7%.

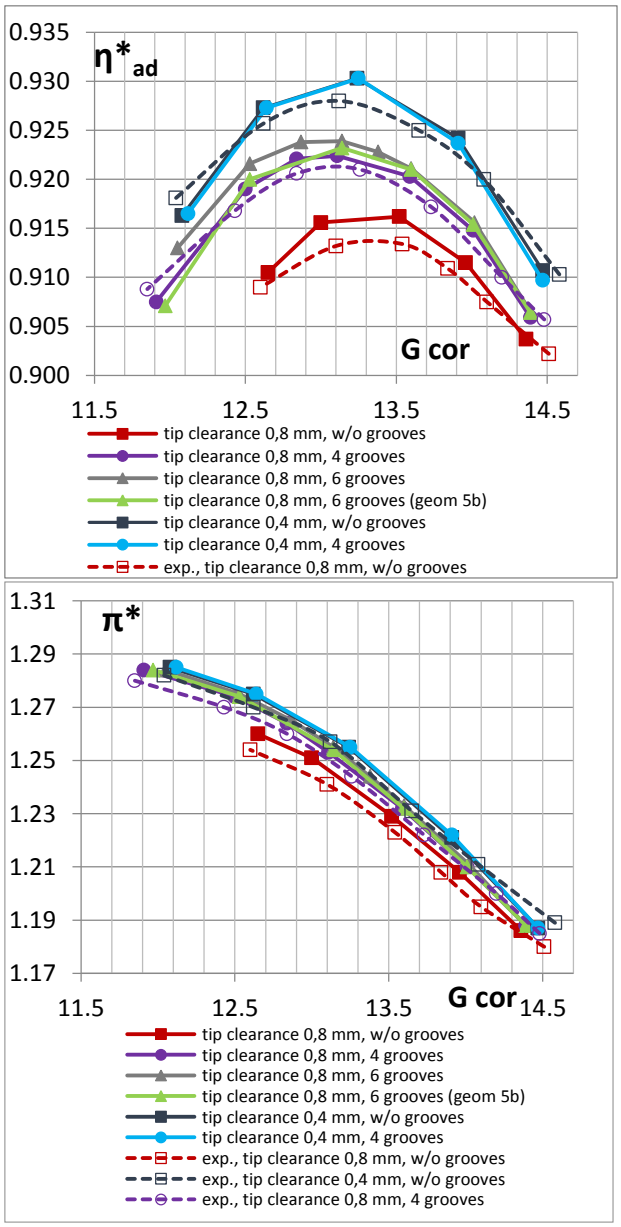

Fig. 6. Integral characteristics of the stage without the outlet guide vanes (IGV + R)

Figure 7 shows integral characteristics of the D-77M stage without the tandem stator found numerically using the NLH method. The purpose of these calculations was validation of data calculated by the "mixing plane" method. The NLH method was more compute-intensive and time consuming, so we restricted ourselves

to the study of only one casing treatment configuration.

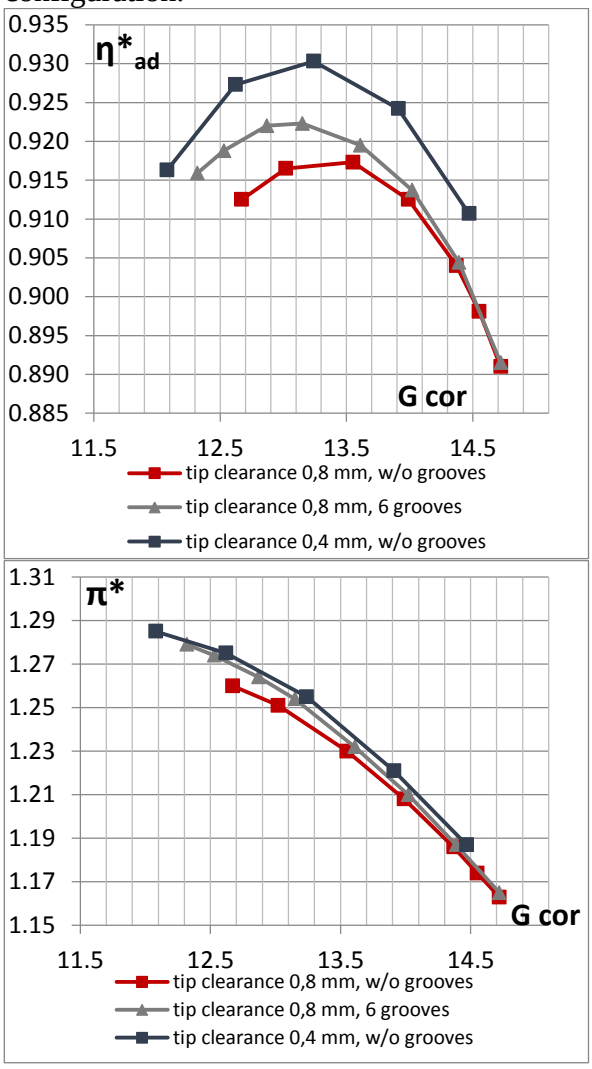

Fig. 7. Integral characteristics of the stage without the outlet guide vanes (IGV+R)

Figure 8 shows integral characteristics of the D-77M stage in IGV+ R+SII configuration found numerically using the "mixing plane" interface. Just as for an incomplete stage, casing treatments of studied configurations had no visible effect on integral characteristics of the stage at nominal tip clearance. Twice as large tip clearance resulted in a decrease in efficiency by 1.5%. Application of casing treatments made possible to increase efficiency by 0.5%, but have no influence on stall margin. Experimental characteristics for the full stage were not found because the initial tandem stator failed to meet the requirements. It has been re-designed and today is in the process of manufacturing. Acquisition of experimental data for the complete stage will be the next step in this work.

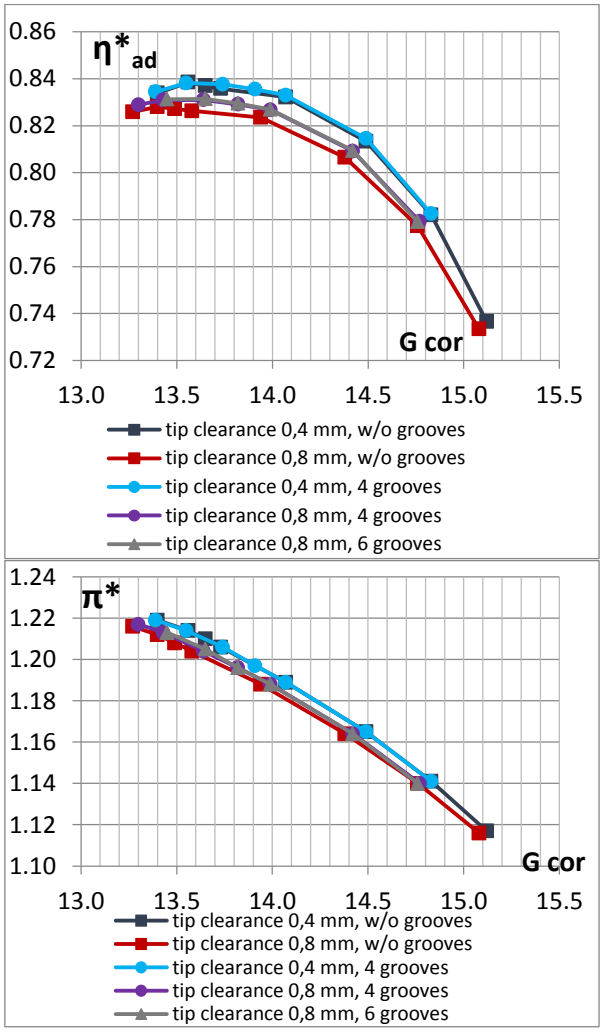

Fig. 8. Integral characteristics of the full stage (IGV+R+SII)

Figure 9 shows distributions of the averaged axial velocity component and streamlines near stall in smooth wall configuration received using mixing plane interface. The points presented for groove configurations have similar mass flow rate. When the tip clearance is 0.4 mm, the reverse flow area is narrow and located at the blade tip, very close to the leading edge. An increase in the tip clearance up to 0.8 mm results in an extended in radial height reverse flow area. Stall occurrence is directly dependant on dimensions and position of the reverse-flow area caused by leakages in the tip clearance. In this case stall was not like a spike; it occurred when a detached bubble got close to the leading edge but not reaching it. The casing treatment installation made possible to shift the detached

bubble from the leading edge, thereby delaying the stall. The circumferential grooves considerable reduce dimensions of this area. A single area splits into a number of smaller spots located under the grooves. Therefore, stall margin can be improved by controlling an increase of the reverse-flow area and its position with an increase in the tip clearance.

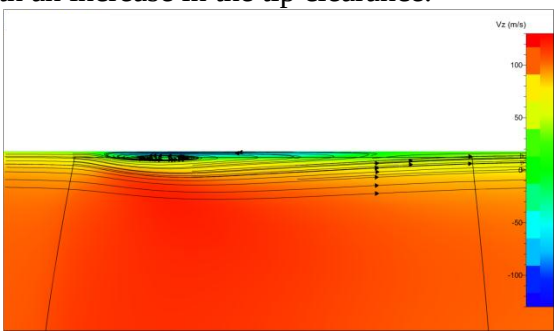

a) IGV+R, tip clearance = 0.4 mm, w/o CT

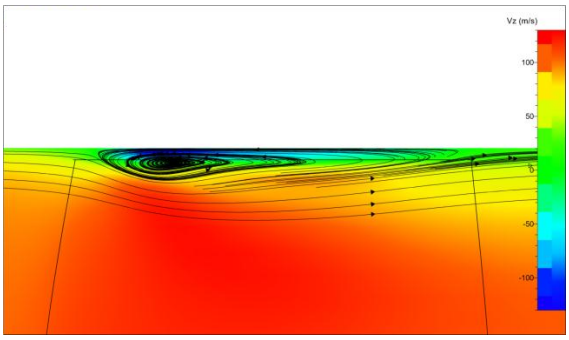

b) IGV+R, tip clearance = 0.8 mm, w/o CT

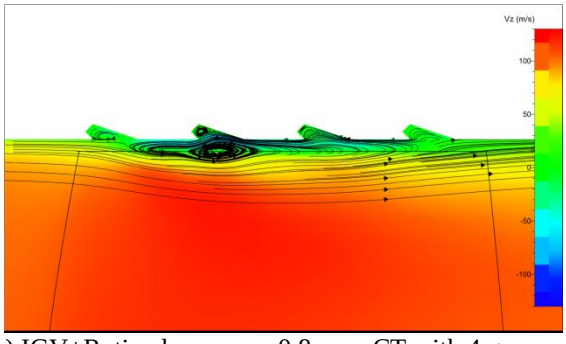

c) IGV+R, tip clearance = 0.8 mm, CT with 4 grooves

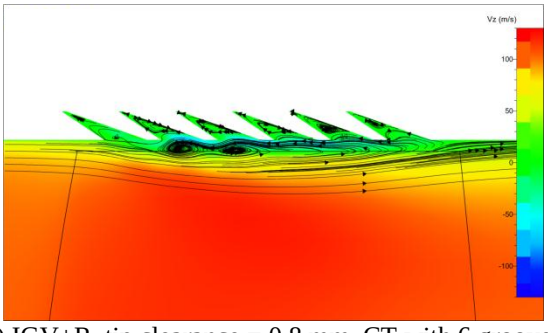

d) IGV+R, tip clearance = 0.8 mm, CT with 6 grooves

Fig. 9. Distribution of the axial velocity component averaged in the circumferential direction; meridional section; near stall; mixing plane interface

The reverse-flow area at the design point (see Fig. 10) is smaller and shifted towards the blade chord center. Higher efficiency of 6 grooves can be attributed to the fact that more clustered grooves split vortex into a number of smaller ones. Nevertheless, the CT with 4 grooves also has a positive effect.

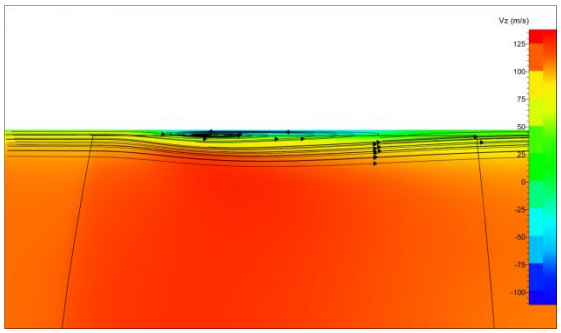

a) IGV+R, tip clearance = 0.4 mm, w/o CT

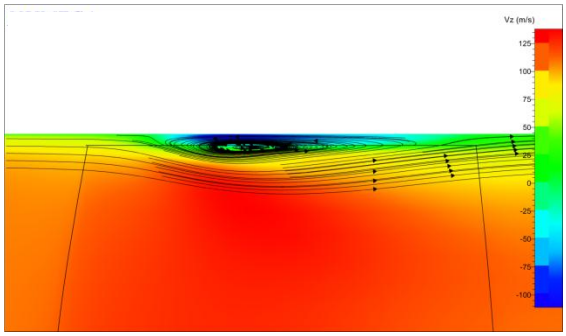

b) IGV+R, tip clearance = 0.8 mm, w/o CT

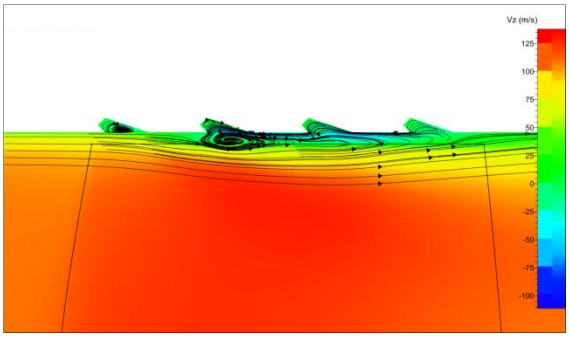

c) IGV+R, tip clearance = 0.8 mm, CT with 4 grooves

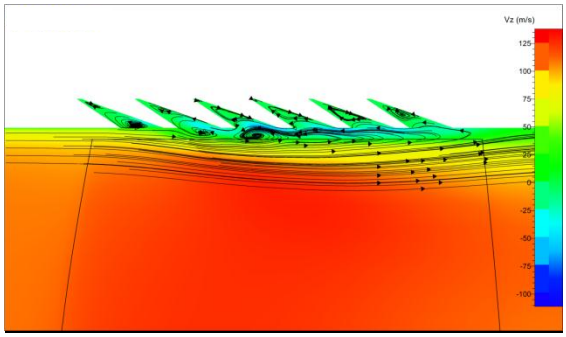

d) IGV+R, tip clearance = 0.8 mm, CT with 6 grooves

Fig. 10. Distribution of the axial velocity component averaged in the circumferential direction; meridional section; near design; mixing plane interface

Figure 11 shows relative Mach number distributions in the blade-to-blade section at 0.97% height of the channel found using the "mixing plane" interface. This section is located lower than the tip clearance and it was chosen because the casing treatment effect in this section was most noticeable. A stagnation area with low relative Mach numbers was located on the blade pressure side. Average value of the relative Mach number in this area was 0.398 at the nominal clearance. An increase in the tip clearance by 2 times resulted in a decreased average value - 0.293 (by 26% lower). Application of 4 and 6 grooves casing treatments made possible to increase the average Mach number value to 0.41 (by 3% higher), and 0.407 (by 2% higher), thereby eliminating the negative effect of an increase in the tip clearance.

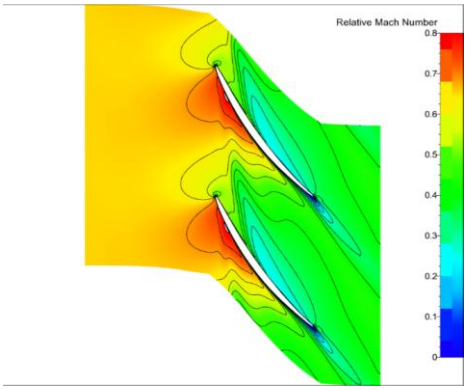

a) IGV+R, tip clearance = 0.4 mm, w/o CT

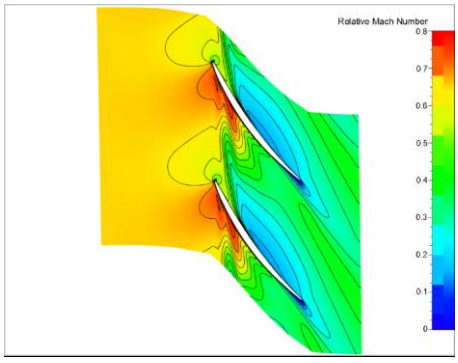

b) IGV+R, tip clearance = 0.8 mm, w/o CT

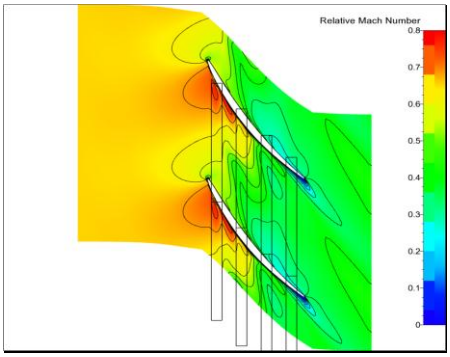

c) IGV+R, tip clearance = 0.8 mm, CT with 4 grooves

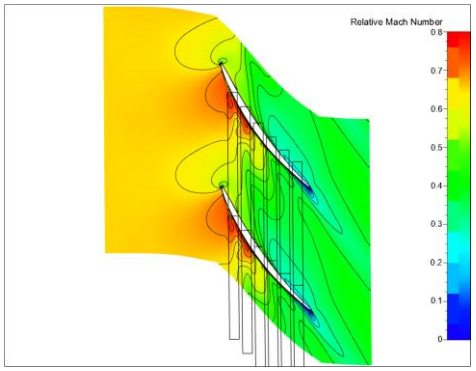

d) IGV+R, tip clearance = 0.8 mm, CT with 6 grooves

Fig. 11. Distribution of Mach numbers in relative CS; blade-to-blade section at 0.97h height; near stall; mixing plane interface

Figure 12 shows the leakage vortex structure in the tip clearance. The version w/o CT shows that vortex is coming from the leading edge. The version with 4 grooves shows that vortex intensity is noticeably lower and its trajectory is located closer to the blade suction side, i.e. in a good agreement with previous studies [9]. Application of circumferential groove casing treatments reduced blockage at the tip; mass air flow increased by 1.2%, while mass air flow through the tip clearance decreased by 0.2%.

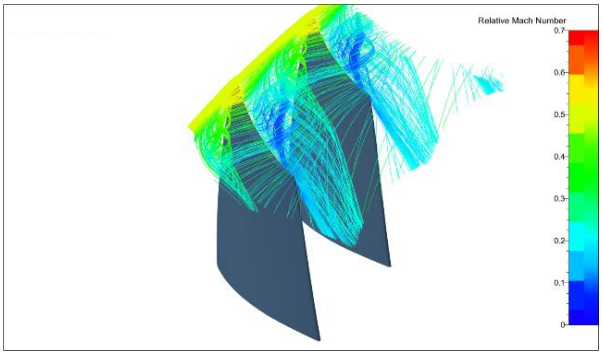

a) IGV+R, tip clearance= 0.8 mm, w/o CT

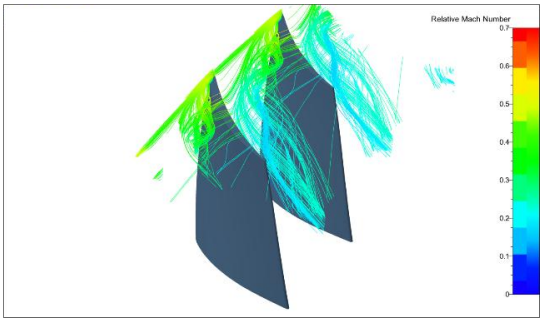

b) IGV+R, tip clearance= 0.8 mm, CT with 4 grooves

Fig. 12. Structure of leakage vortex in the tip clearance; near stall; mixing plane interface

Figure 13 shows that leakage in the tip clearance results in occurrence and changes in the stagnation zone on the blade pressure side (at the tip). The position of this zone coincides with the leakage vortex trajectory. The circumferential grooves provide a considerable reduction of this zone by decreasing leakage intensity in the tip clearance.

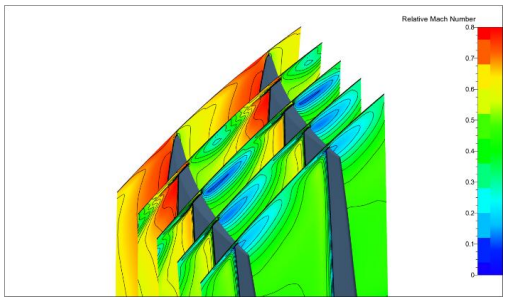

a) IGV+R, tip clearance = 0.8 mm, w/o CT

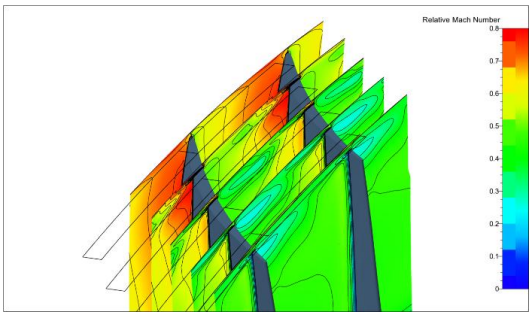

b) IGV+R, tip clearance= 0.8 mm, CT with 4 grooves

Fig. 13. Distribution of Mach numbers in the relative coordinate system; sections in the blade channel; near stall; mixing plane interface

An increase in leakage vortex intensity leads to entropy production (Fig. 14) and losses generation. Application of the CT provides a considerable decrease in entropy production, and, as a consequence, higher efficiency.

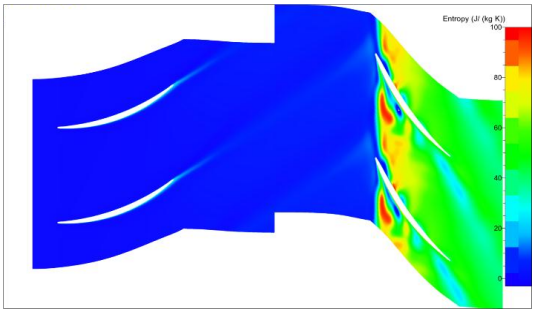

a) IGV+R, tip clearance= 0.8 mm, w/o CT

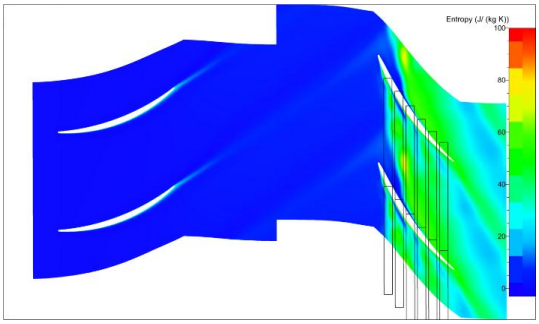

b) IGV+R, tip clearance = 0.8 mm, CT with 4 grooves

Fig. 14. Entropy distribution; blade-to-blade section at 0.97h height; near stall; NLH method

Figure 15 shows the relative Mach number distribution at the tip for the full stage. The stagnation zone in the tail part of the rotor blade is considerably smaller than for the stage version without the stator. However, the circumferential grooves almost completely remove this zone. Leakage vortex at the leading edge is re-structured. It is worth noting that casing treatments of this type have weak effect on flow in the next rows.

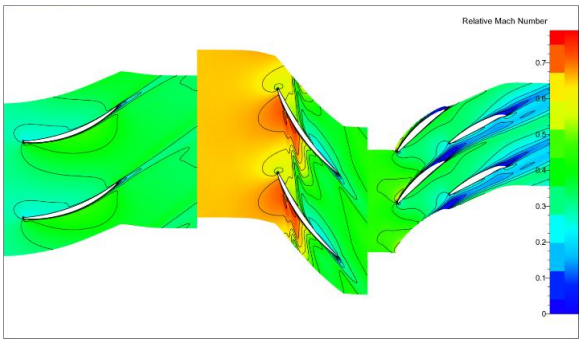

a) IGV+R+SII, tip clearance= 0.8 mm, w/o CT

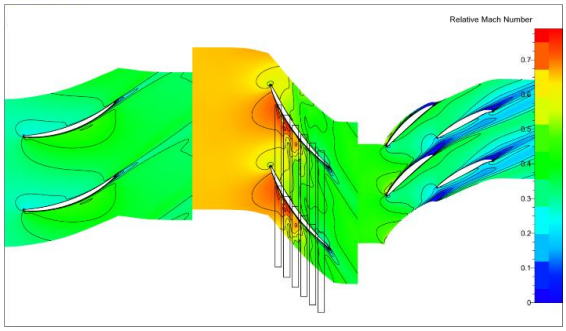

b) IGV+R+SII, tip clearance= 0.8 mm, CT with 6 grooves

Figure 15 – Distribution of Mach numbers in the relative coordinate system; blade-to-blade section at 0.97h height; full stage; near stall

A distinctive feature of the last stage in a heavy-loaded HPC is a powerful wake coming from previous stages. Unsteady interaction between this wake-generated disturbance and the rotor considerably changes the flow pattern; therefore, effectiveness of casing treatments in this case is questionable. In this work, the wake-generated disturbance is numerically simulated by decreasing the total pressure at the inlet by 10% (Fig. 16); it is shown that even in this case the circumferential grooves have a positive effect on performance of the last compressor stage. Rotation of inlet non-uniformity will be considered later.

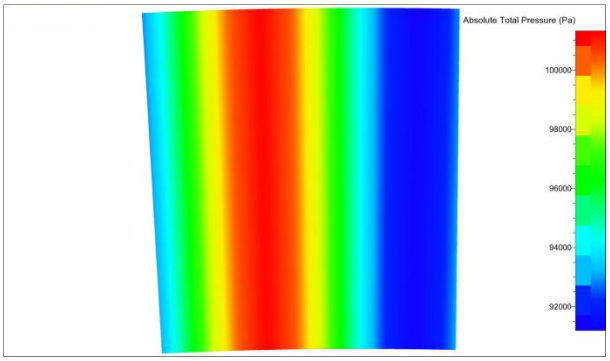

Figure 16 – Shape of the inlet wake

Figure 17 represents comparison of integral characteristics of the D-77M stage in the configuration without outlet stator SII at 0.8 mm tip clearance, obtained by NLH method in uniform inlet flow conditions and in conditions of total pressure drop, simulating circumferential flow distortion. In conditions of inlet flow nonuniformity casing treatment demonstrates the same effect: the efficiency increased insignificantly, surge margin increased on 4.6%.

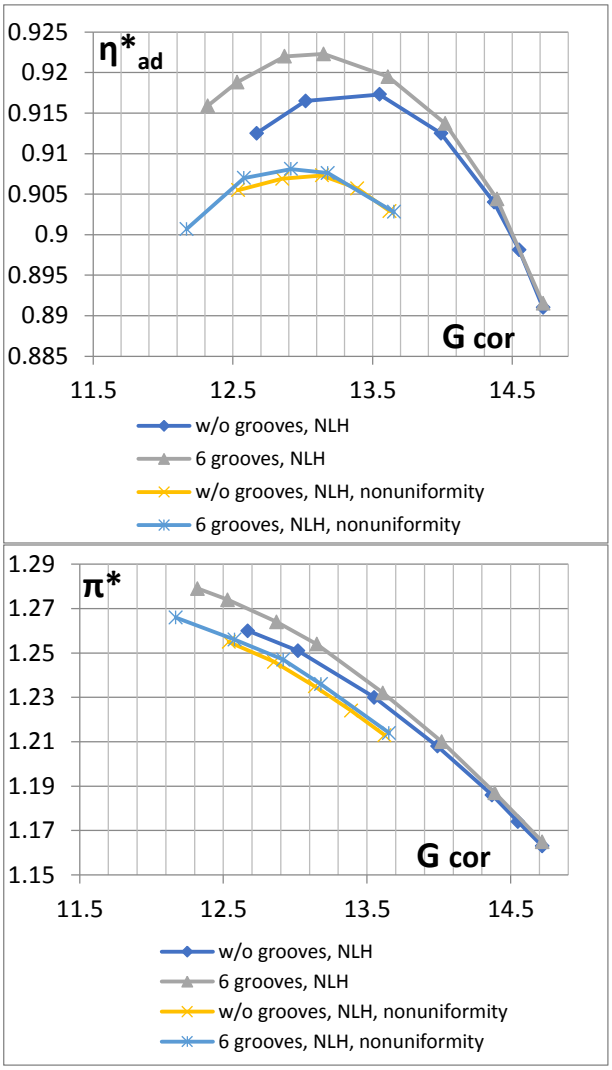

Figure 17 – Integral characteristics of the stage without the stator (IGV + R), tip clearance= 0.8 mm, NLH method, nonuniformity

CONCLUSION

1. The algorithm and the mathematical model are developed on the basis of 3D viscous flow calculation procedure for numerical simulation of 3D effects in a large-scale model of a typical HPC last stage - the D-77M stage with circumferential groove casing treatments.
2. Steady and unsteady flow fields in blade channels are found for the D-77M stage with a smooth flow path and with circumferential groove casing treatments.
3. The comparison of calculated and experimental data shows their acceptable matching for the stage version with a smooth flow path and d_{tip}= 0.4 mm or d_{tip} =

0.8 mm tip clerances as well as for the stage with four grooves and d_{tip} = 0.8 mm tip clearance. Maximum deviation for efficiency was 0.5% at all analyzed values of the tip clearance; maximum deviation for total pressure ratio (π^*) was 0.7%

4. 3D viscous turbulent flows in the D-77M stage with a smooth flow path and various versions of circumferential grooves are calculated for the stage with and without outlet guide vanes. When the tip clearance is 0.4 mm, the circumferential grooves have no effect on performance of the stage in both versions. When the tip clearance is 0.8 mm, the effect of circumferential grooves becomes noticeable. The CT configuration with 6 triangular grooves is most effective. Stall margin of this stage without stator increases by 7% and maximum efficiency - by 0.8% for this groove shape. The stage in the configuration IGV + R+SII with 6 grooves provides an increase in efficiency by 0.4% and no changes in stall margin.
5. It is shown that circumferential grooves make possible to reduce the leakage vortex intensity in the tip clearance, thereby improving the streamlining of blades at the tip and increasing stall margin.
6. This work was carried out in an effort to develop methods and technologies aiming at an improvement the last compressor stage performance (including an increase in stall margins), as well as a reduction of sensitivity of last compressor stage performance to changes in rotor tip clearances. Next steps in this work will be a numerical study the effect of inlet rotating non-uniformity and an experimental study of the full stage.

References

[1] Dr. H. Scheugenpflug and Dr. Aspi Wadia, 2013, "Technologies for the Next Engine Generation GE Aviation", *Proceedings of XXI International Symposium on Air Breathing Engines*, Seoul, South Korea, Invited lecture ISABE2013-1007.

[2] P.S. Prahst, S. Kulkarni, Ki H. Sohn, 2015, "Experimental results of the first two stages of an advanced transonic core compressor under isolated and multi-stage conditions**"** *Proceedings of ASME Turbo Expo 2015*, Paper No. GT2015-42727.

[3] D.P. Lurie, A. Breeze-Stringfellow, 2015, "Evaluation of experimental data from a highly loaded transonic compressor stage to determine loss sources", *Proceedings of ASME Turbo Expo 2015*, Paper No. GT2015-42526.

[4] V.I. Mileshin, 2013, "Numerical and experimental investigation of bypass fan stage models and high loaded compressor stages for development of new fan and high pressure compressor for advanced engines". *Proceedings of 10 European Turbomachinery Conference*, Lappeenranta, Finland, Invited lecture.

[5] V.I. Mileshin, 2013, Key-note speech "Challenges in fan and high pressure compressor development". *Proceedings of XXI International Symposium on Air Breathing Engines*, Busan, South Korea, Paper No. ISABE2013-1003.

[6] V.I. Mileshin, I.K. Orekhov, V.A. Fateyev, S.K. Shchipin, 2007, "Effect of tip clearance on flow structure and integral performances of six-stage HPC", *Proceedings of XVIII International Symposium on Air Breathing Engines*, Beijing, China, Paper No. ISABE-2007-1179.

[7] V.I. Mileshin, N.M. Savin, P.G. Kozhemyako, Ya.M. Druzhinin, 2014, "Numerical and experimental analysis of radial clearance influence on rotor and stator clocking effect by example of model high loaded two stage compressor", *Proceedings of ASME Turbo Expo 2014*, Dusseldorf, Germany, Paper No. GT2014-26345.

[8] F.Sh. Gelmedov, V.I. Mileshin, P.G. Kozhemyako, I.K. Orekhov, 2014, "Stall margin improvement in three-stage low pressure compressor by use of slot type casing treatments", *Proceedings of ASME Turbo Expo 2014*, Dusseldorf, Germany Paper No. GT2014-26298.

[9] Victor Mileshin, Igor Brailko, Andrew Startsev "Application of casing circumferential grooves to counteract the influence of tip clearance" *Proceedings of ASME Turbo Expo 2008*, No. GT2008-51147.

[10] Shraman Narayan Goswami, Prof. M. Govardhan, 2016, "Effect of sweep on performance of an axial compressor with casing grooves", Proceedings of ASME Turbo Expo 2016, Seoul, South Korea, Paper No. GT2016-56045.

[11] Juan Du, Fan Li, Jichao Li, Ning Ma, Feng Lin, Jingyi Chen, 2015, "A study of performance and flow mechanism of a slot-groove hybrid casing treatment in a low-speed compressor" *Proceedings of ASME Turbo Expo 2015*, Montreal, Canada, Paper No. GT2015-43920.

[12] Wilke, I., and Kau, H.-P., 2003, "A Numerical Investigation of the Flow Mechanisms in a HPC Front Stage with Axial Slots", *Proceedings of ASME Turbo Expo 2003*, Atlanta, USA, Paper No. GT2003-38481.

[13] Beheshti, B.H., Teixeira, J.A., Ivey, P.C., Ghorbainian, K., Farhanieh, B., 2004, "Parametric

Study of Tip Clearance – Casing Treatment on Performance and Stability of a Transonic Axial Compressor", *Proceedings of ASME Turbo Expo 2004*, Vienna, Austria, Paper No. GT2004-53390.

[14] Muller, M.W., Schiffer, H.-P. and Hah C., 2007, "Effect of Circumferential Grooves on the Aerodynamic Performance of an Axial Single-Stage Transonic Compressor", *Proceedings of ASME Turbo Expo 2007*, Montreal, Canada, Paper No. GT2007-27365.

[15] Rabe, D.C., and Hah, C., 2002, "Application of Casing Circumferential Grooves for Improved Stall Margin in a Transonic Compressor", *Proceedings of ASME Turbo Expo 2002*, Amsterdam, The Netherlands, Paper No. GT2002-30641.

[16] Shabbir, A., and Adamzyk J.J, 2004, "Flow Mechanism for Stall Margin Improvement due to Circumferential Casing Grooves on Axial Compressor", *Proceedings of ASME Turbo Expo 2004*, Vienna, Austria, Paper No. GT2004-53903.

[17] Georgios Goinis, Christian Voß and Marcel Aulich, 2013, "Circumferential grooves for a modern transonic compressor: aerodynamic effects, benefits and limitations." *Proceedings of 10 European Turbomachinery Conference*, Lappeenranta, Finland, Paper No. ETC10-60.

[18] M. Rolfes, M. Lange and K. Vogeler, 2015, "Experimental investigation of circumferential groove casing treatments for large tip clearances in a low speed axial research compressor" *Proceedings of ASME Turbo Expo 2015*, Montreal, Canada, Paper No. GT2015.

[19] Hao Guang Zhang, Feng Tan, Yan Hui Wu, Wu Li Chu, Wei Wang, Kang An, 2016, "Experimental and numerical investigation of effect of centeroffset degree on compressor stability with circumferential grooved casing treatment" *Proceedings of ASME Turbo Expo 2016*, Seoul, South Korea, Paper No. GT2016-56757.

[20] Cevik, M. et al., 2016, "Casing Treatment for Desensitization of Compressor Performance and Stability to Tip Clearance", ASME J. Turbomach., **Vol. 138**.

[21] Erler, E. et al., 2015, "Desensitization of Axial Compressor Performance and Stability to Tip Clearance Size ", ASME J. Turbomach., **Vol. 138**.

[22] Hirsch Ch., 1990, Numerical Computation of Internal and External Flows. Volume 2. // John Wiley & Sons.

[23] Hirsch Ch., 2012, Non-Deterministic Methodologies for Uncertainty quantification in turbomachinery CFD, Numeca international, Brussels. Pannel session. *Proceedings of ASME Turbo Expo 2012*, Copenhagen, Denmark.

[24] He, L. and Ning, W., 1998, "Efficient Approach for Analysis of Unsteady Viscous Flows in Turbomachines", AIAA Journal, **Vol. 36**, No. 11.

[25] Van Zante et al., 1999, "Recommendations for Achieving Accurate Numerical Simulation of Tip Clearance Flows in Transonic Compressor Rotors", *Proceedings of ASME Turbo Expo*, Paper 99-GT-390.

Contact Author Email Address

Mailto: corresponding author:
mileshin@ciam.ru

Copyright Statement